

## Error Counting in a Quantum Error-correcting Code and the Ground-State Energy of a Spin Glass

Hidetoshi NISHIMORI and Peter SOLLICH<sup>1</sup>

*Department of Physics, Tokyo Institute of Technology, Oh-okayama, Meguro-ku, Tokyo 152-8551*  
<sup>1</sup>*Department of Mathematics, King's College London, Strand, London WC2R 2LS, United Kingdom*

(Received May 14, 2004)

Upper and lower bounds are given for the number of equivalence classes of error patterns in the toric code for quantum memory. The results are used to derive a lower bound on the ground-state energy of the  $\pm J$  Ising spin glass model on the square lattice with symmetric and asymmetric bond distributions. This is a highly non-trivial example in which insights from quantum information lead directly to an explicit result on a physical quantity in the statistical mechanics of disordered systems.

KEYWORDS: quantum information, quantum memory, toric code, spin glass,  $\pm J$  model, ground-state energy  
 DOI: 10.1143/JPSJ.73.2701

### 1. Introduction

In a recent paper, Dennis–Kitaev–Landall–Preskill (DKLP)<sup>1)</sup> showed that error correction in the toric code for stable storage of quantum information is closely related to the phase transition between ferromagnetic and paramagnetic phases in the two-dimensional  $\pm J$  Ising model of spin glasses. This is remarkable in that it paves a way for transferring results, concepts and insights between the two at first sight unrelated domains of quantum error correction and spin glasses, and provides the motivation for the present work.

An important aspect of the toric code is that it has a finite error threshold; this is the critical value of error probability per qubit beyond which it is impossible to correct errors in the thermodynamic (large system-size) limit. Thus, for error rates larger than the threshold, the encoded quantum information is lost. It is therefore necessary to estimate the precise value of the error threshold for, *e.g.*, the design of hardware of quantum memory. DKLP have shown that this error threshold is equal to the probability of antiferromagnetic bonds at the multicritical point in the phase diagram of the  $\pm J$  Ising model on the square lattice.

We do not discuss the value of error threshold itself in the present paper.<sup>1–3)</sup> We instead strive to clarify a closely related problem of the structure of error patterns underlying a characteristic feature of the toric code, *degeneracy*, by deriving bounds on the number of equivalent error patterns. These bounds are shown to be related to the information-theoretical entropy of the distribution of frustrated plaquettes in the  $\pm J$  Ising model. It will also be shown that a lower bound on the ground-state energy of the  $\pm J$  Ising model can be obtained from the bounds derived for the toric code.

We outline the link between spin glasses and quantum error correcting codes in §2. Errors are detected by measurement of a syndrome, from which the underlying error pattern is to be inferred and then corrected. Due to the nature of quantum encoding in the toric code, however, many error patterns are equivalent (degenerate), and it is sufficient to infer the equivalence class of the true error pattern, not the precise pattern itself. In §3 we count the number of syndromes  $D$  and the total number of equivalence classes  $C$ , which is an easy task. The hard part is counting the number of equivalence classes  $C(p)$  containing error

patterns with a given fraction  $p$  of errors. We first ignore the issue of degeneracy, and count error patterns instead of equivalence classes, from which upper bounds on  $C(p)$  are derived in §4.1. Lower bounds are discussed in §4.2 and 4.3. These bounds are summarized in §4.4. One of the lower bounds involves the ground-state energy of the  $\pm J$  Ising model, and this fact is used in §4.5 to derive a lower bound on the latter ground-state energy. The results are summarized and discussed in §5.

### 2. Toric Code and Spin Glass

It is useful to first sketch the connection between toric quantum codes and two-dimensional spin glasses, following DKLP,<sup>1)</sup> since most of the readers may be unfamiliar with this relatively new interdisciplinary field.

#### 2.1 Encoding in the toric code

Consider a square lattice with  $N = L^2$  sites and  $n = 2N$  bonds labelled by  $b = (ij)$  and connecting nearest-neighbour sites  $i$  and  $j$ ; toroidal boundary conditions are used so that bonds on a boundary connect to the opposite side of the lattice. The toric code comprises  $n$  quantum (spin-1/2) spins located on the bonds of the lattice. We call the local Pauli operators  $X_b$ ,  $Y_b$  and  $Z_b$ . In the  $Z$ -basis of the state space, each basis vector  $|z\rangle = \{|z_b\rangle\}$  is specified by the  $z$ -components  $z_b = \pm 1$  of all spins. The Pauli operators then act as  $Z_b|\dots z_b \dots\rangle = z_b|\dots z_b \dots\rangle$  and  $X_b|\dots z_b \dots\rangle = |\dots -z_b \dots\rangle$  so that  $X_b$  effectively just flips the spin at  $b$ ; also,  $Y_b = iX_bZ_b$ .

Quantum states are vulnerable to decoherence, and robustness should be introduced to protect quantum information. Quantum error correction is a powerful method for this purpose, in which one encodes quantum information by mapping it to another (redundant) set of quantum states. Specifically, in the toric code, one maps the state space of two logical qubits that are to be encoded onto a  $2^2 = 4$ -dimensional subspace (the “code space”) of the spin system’s  $2^n$ -dimensional state space. This mapping is redundant because  $n$  qubits are used to represent 2 qubits. A basis  $|\psi_0\rangle, \dots, |\psi_3\rangle$  for the code space can be defined as

$$|\psi_i\rangle \propto \sum_{z \in \mathcal{C}_i} |z\rangle, \quad (1)$$

where  $\mathcal{C}_i$  denotes a class of states (*equivalence class*) to be

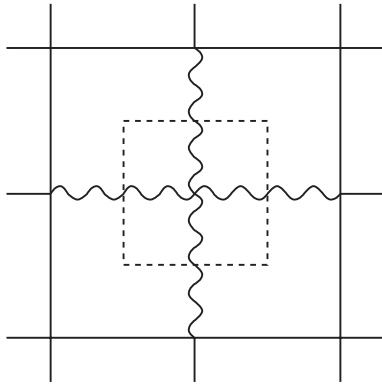


Fig. 1. Example of a cycle. Full lines represent bonds with  $z_b = 1$  and wavy lines are for  $z_b = -1$ . Dual bonds to  $z_b = -1$  form a closed loop (shown dotted).

defined shortly. The sum here runs over states  $|z\rangle$  which form *cycles* within an equivalence class. This means that out of the four bonds  $b(P)$  around each lattice plaquette  $P$  an even number are negative ( $z_b = -1$ ). A cycle  $|z\rangle$  is thus an eigenstate with eigenvalue 1 of all the operators  $Z_P = \prod_{b(P)} Z_b$ . Geometrically,  $|z\rangle$  is a cycle if the duals to its negative bonds form closed loops on the dual lattice (see Fig. 1).

2.2 Equivalence class

Cycles are called equivalent if they can be locally deformed into each other, by repeatedly flipping all spins around some plaquette of the dual lattice. As illustrated in Fig. 2, this corresponds on the original lattice to applying a product of operators of the form  $X_j = \prod_{b(j)} X_b$ , where the

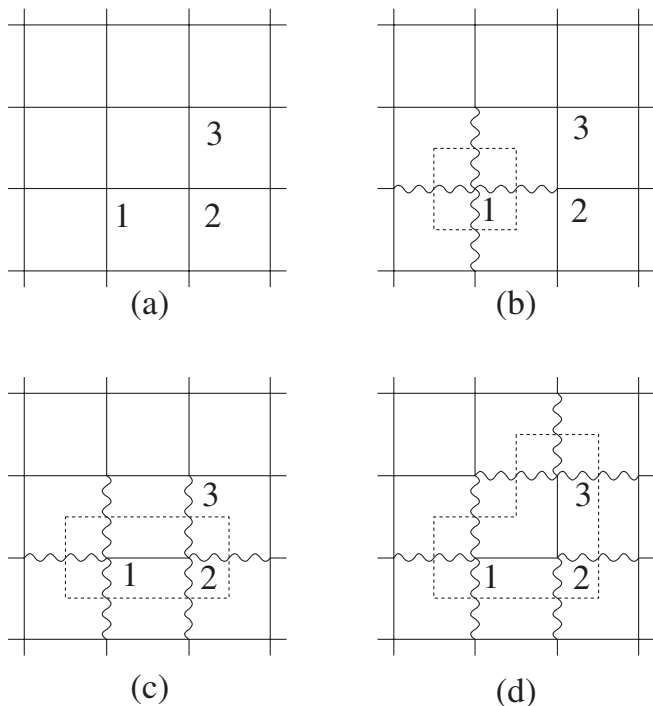


Fig. 2. Four equivalent cycles. Full, wavy and dotted lines have the same meaning as in Fig. 1. Application of  $X_1$  to (a) gives (b); similarly, (c) and (d) are obtained from (a) by applying  $X_2X_1$  and  $X_3X_2X_1$ , respectively.

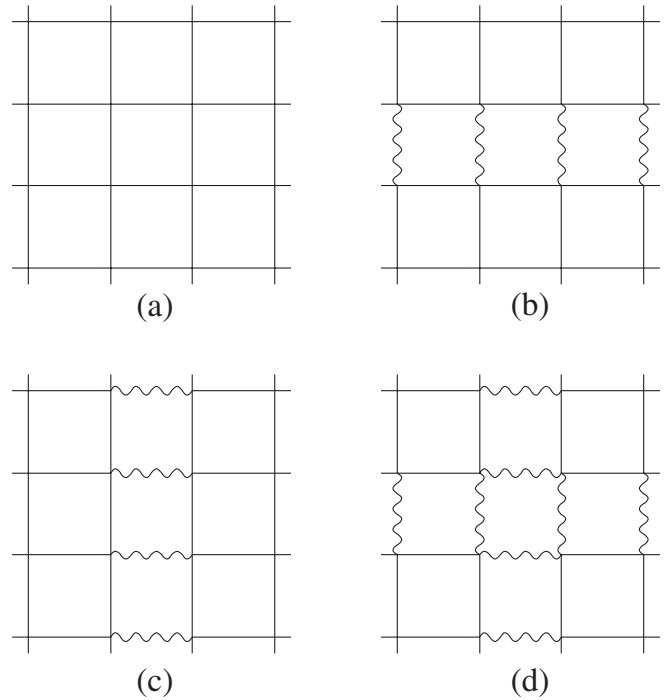


Fig. 3. Representative cycles of four different classes,  $\mathcal{C}_0, \mathcal{C}_1, \mathcal{C}_2$  and  $\mathcal{C}_3$  in (a), (b), (c) and (d), respectively.

$b(j)$  are the four bonds meeting at site  $j$ . It is then easy to see that there are exactly four equivalence classes of cycles, denoted  $\mathcal{C}_0, \dots, \mathcal{C}_3$ :  $\mathcal{C}_0$  contains all the trivial cycles, which are equivalent to the empty cycle state  $|\{z_b = 1\}\rangle$ .  $\mathcal{C}_1$  and  $\mathcal{C}_2$  collect cycles equivalent to a single loop winding across the lattice boundary in the horizontal and vertical directions respectively, and  $\mathcal{C}_3$  those with both a horizontal and a vertical loop (Fig. 3). In (1), what is meant is that for each  $|\psi_i\rangle$  the sum runs over all cycle states  $|z\rangle$  in the equivalence class  $\mathcal{C}_i$ . This implies in particular that the  $|\psi_i\rangle$  are invariant under the action of any of the operators  $Z_P$  and  $X_j$ : the  $Z_P$  leave each cycle state  $|z\rangle$  invariant, and the  $X_j$  only permute cycle states within an equivalence class,

$$Z_P|\psi_i\rangle = X_j|\psi_i\rangle = |\psi_i\rangle. \tag{2}$$

In the large- $N$  limit, the toric code has zero code rate  $R$ : it encodes  $k = 2$  qubits using  $n = 2N$  qubits, so that  $R = k/n = 1/N \rightarrow 0$ . The point of this highly redundant encoding is to allow for the correction of errors arising from decoherence caused by the interaction of the quantum state with its environment. An error introduced in this way corresponds to a product of Pauli operators  $X, Y, Z$  acting on some of the quantum spins. Because of  $Y = iXZ$ ,  $Y$ -errors can be treated as combinations of  $X$ - and  $Z$ -errors. We write a state with  $X$ -errors on a set of bonds  $\delta_x$  and  $Z$ -errors on  $\delta_z$  as

$$|\tilde{\psi}_i\rangle = \left( \prod_{b \in \delta_x} X_b \prod_{b \in \delta_z} Z_b \right) |\psi_i\rangle. \tag{3}$$

If the product of  $X_b$  and  $Z_b$  on the right-hand side can be represented by a product of  $X_j$  and  $Z_P$  only, then  $|\tilde{\psi}_i\rangle = |\psi_i\rangle$ . In general, however, this is not the case,  $|\tilde{\psi}_i\rangle \neq |\psi_i\rangle$ .

Furthermore, the toric code is in the general class of Calderbank–Shor–Steane (CSS) codes,<sup>4,5</sup> for which the  $X$ - and  $Z$ -errors can be treated separately, without interference

between the corresponding error correction procedures because  $[Z_P, X_j] = 0$  for any  $P$  and  $j$ .<sup>1)</sup> We can therefore focus in the following exclusively on  $X$ -errors, i.e., spin flips.  $Z$ -errors can be discussed separately in the same manner but on the dual lattice.<sup>1)</sup>

### 2.3 Syndrome and error correction

We define an *error pattern*  $\{\tau_b\}$  such that  $\tau_b = -1$  if an  $X$ -error has occurred on bond  $b$  (i.e., if  $b \in \mathcal{E}_x$ ) and  $\tau_b = 1$  otherwise. To diagnose where errors have occurred, one measures all the  $Z_P$ . Without corruption all measured values would be 1 according to (2). The errors give a nontrivial set of measurement values  $\prod_{b(P)} \tau_b = -1$  at those plaquettes around which an odd number of errors have occurred, giving the *syndrome*, the set of plaquettes with measurement value  $-1$ . It should be stressed that the syndrome measurement does not cause any quantum decoherence: From (3), one easily sees—by commuting  $Z_P$  to the right through the various  $X_b$  and using (2)—that even a corrupted state  $|\tilde{\psi}_i\rangle$  is an eigenstate of each  $Z_P$ . Explicitly,  $Z_P|\tilde{\psi}_i\rangle = \pm|\tilde{\psi}_i\rangle$ , with the plus sign when there are an even number of errors around  $P$  and the minus sign otherwise.

One can visualize the error pattern  $\tau$  by drawing the duals to the bonds with  $\tau_b = -1$ ; these form “error chains” ending in “defects”, i.e., plaquettes where the syndrome has detected an error (Fig. 4). The syndrome measurement is therefore highly ambiguous: any error chain  $\tau'$  with the same set of defects as  $\tau$  gives the same syndrome as exemplified in Fig. 4. The condition for this is  $\prod_{b(P)} \tau_b = \prod_{b(P)} \tau'_b$  for all plaquettes  $P$  and hence  $\prod_{b(P)} \tau_b \tau'_b = 1$ : the bonds with  $\tau_i \tau'_i = -1$  form a cycle  $\tau\tau'$  in the sense defined above.

Now assume we have inferred some error pattern  $\tau'$  consistent with the syndrome [e.g., Fig. 4(a)], so that  $\tau\tau'$  is a cycle, where  $\tau$  is the actual error pattern [e.g., Fig. 4(b)]. If we correct errors according to  $\tau'$ , by applying a spin-flip  $X_b$  to all spins with  $\tau'_b = -1$ , this can be viewed as first correcting the errors  $\tau_b$  that actually occurred, followed by a series of spin-flips where  $\tau_b \tau'_b = -1$  [four double lines in Figs. 4(a) and 4(b)]. The first stage recovers the uncorrupted code state  $|\psi_i\rangle$ . If  $\tau\tau'$  is a *trivial cycle* ( $\tau\tau' \in \mathcal{C}_0$ ), then the second stage corresponds to applying a product of operators of the form  $X_j$ . But these leave code states invariant, see (2), so that our error correction was successful. This is a key difference of this *degenerate* quantum code to classical error correction: we do not need to detect all details of the error pattern  $\tau$ , but only its equivalence class (defined as the set of all  $\tau'$  such that  $\tau\tau'$  is a trivial cycle). Error correction

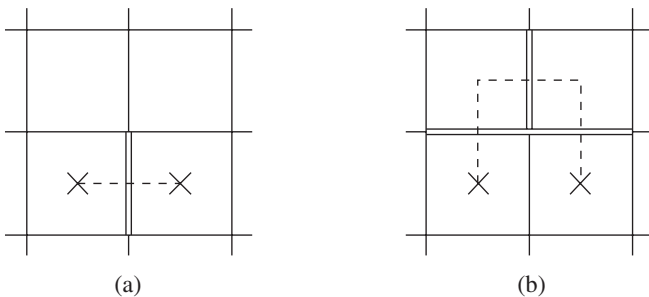


Fig. 4. Error patterns with the same syndrome (crosses). Double lines are bonds where  $\tau_b = -1$ . Error chains are written in dashed lines.

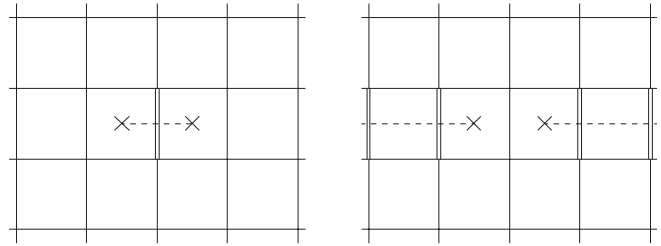


Fig. 5. Non-equivalent error patterns with the same syndrome.

according to  $\tau'$  will be unsuccessful, on the other hand, if  $\tau$  and  $\tau'$  are non-equivalent, i.e., if  $\tau\tau'$  is a *nontrivial cycle* like Fig. 5: the second stage from above then mixes up the basis vectors of different code spaces.

### 2.4 Spin-glass representation

We can now relate the decoding task to a spin glass problem. The condition that  $\tau\tau'$  is a trivial cycle can be written as  $\tau'_{ij} = \tau_{ij}\sigma_i\sigma_j$  if we revert to denoting each bond  $b$  by its end points  $i$  and  $j$ . Here the  $\sigma_i = \pm 1$  are classical spin variables. Then the second (conceptual) stage of error correction discussed above would consist of the application of an operator  $X_j$  for each site where  $\sigma_j = -1$  (the central site in the case of Fig. 4). Assuming that errors were generated independently and with probability  $p$  on each bond  $b$ , we assign an overall probability

$$P(\tau') = \prod_{(ij)} (1-p)^{(1+\tau'_{ij})/2} p^{(1-\tau'_{ij})/2} = [p(1-p)]^{n/2} \exp\left(K_p \sum_{(ij)} \tau'_{ij}\right) \quad (4)$$

to any error chain  $\tau'$ ; here we have defined  $K_p = \frac{1}{2} \ln[(1-p)/p]$ . The total probability for error chains  $\tau'$  which lead to successful error correction is therefore proportional to

$$Z_0 = \sum_{\tau': \tau\tau' \in \mathcal{C}_0} \exp\left(K_p \sum_{(ij)} \tau'_{ij}\right) = \sum_{\sigma} \exp\left(K_p \sum_{(ij)} \tau_{ij}\sigma_i\sigma_j\right). \quad (5)$$

This is the partition function of an Ising  $\pm J$  spin glass with local interaction strengths  $J_{ij} = K_p \tau_{ij}$ ; the relation between  $K_p$  and  $p$  implies that the system is on the so-called Nishimori line (NL).<sup>6,7)</sup> If the actual error pattern  $\tau$  was indeed generated according to the assumed probability weight (4), each bond in (5) is ferromagnetic with probability  $1-p$  ( $\tau_{ij} = 1$ ) and antiferromagnetic otherwise.

The total probability for error chains  $\tau'$  which lead to *faulty* error correction has the same form as (5), but with modified boundary conditions. For example, any  $\tau'$  such that  $\tau\tau' \in \mathcal{C}_2$  can be written as  $\tau'_{ij} = \tau_{ij}\sigma_i\sigma_j$  with the convention that all bonds along, say, the left boundary of the lattice are inverted. This corresponds to the use of antiperiodic boundary conditions in the left–right direction when evaluating the spin products  $\sigma_i\sigma_j$ . The total probability weight  $Z_2$  for error chains  $\tau'$  with  $\tau\tau' \in \mathcal{C}_2$  is therefore a partition function of the form (5) with these modified boundary conditions; in  $Z_0$  we had implicitly assumed periodic boundary conditions. Similarly  $Z_1$  and  $Z_3$  correspond to

the partition functions for antiperiodic boundary conditions in the top–bottom direction, and in both left–right and top–bottom directions.

Combining the above results, we conclude that our total probability of inferring from the syndrome an error chain  $\tau'$  which leads to successful error correction is  $\mathcal{Z}_0/(\mathcal{Z}_0 + \mathcal{Z}_1 + \mathcal{Z}_2 + \mathcal{Z}_3)$  and close to unity as long as  $\mathcal{Z}_0 \gg \mathcal{Z}_k$  for  $k = 1, 2, 3$ . This condition is met if  $p$  is small enough so that we are in the ferromagnetic phase of the spin system defined by (5): the existence of domain boundaries then implies for the free energies  $F_i = -T \ln \mathcal{Z}_i$  that  $F_k - F_0$  ( $k = 1, 2, 3$ ) is positive and of order  $L$ , thus  $\mathcal{Z}_0 \gg \mathcal{Z}_1, \mathcal{Z}_2, \mathcal{Z}_3$ . In the paramagnetic phase, on the other hand,  $F_k - F_0 = \mathcal{O}(1)$  and there will be a nonzero probability for error correction to fail. In summary, the toric code can correct errors below an error threshold, i.e., in the range  $0 \leq p \leq p_c$  where the associated  $\pm J$  Ising spin glass on the NL is in its ferromagnetic phase on the square lattice;  $p_c$  is then the location of the multicritical point. We may therefore be able to learn something about the spin glass problem from knowledge about the toric code and *vice versa*. This is our motivation for the present work.

### 3. Simple Number Counting

The argument in the previous section suggests that the numbers of possible syndromes and equivalence classes of error patterns would give important measures of performance of error correction in the toric code. We therefore discuss this problem in the present and next sections.

Let us first count the total numbers of different syndromes and equivalence classes, without specifying the error probability  $p$ . Since at each plaquette the syndrome measurement of  $Z_p$  can give either  $+1$  or  $-1$ , the total number of syndromes is

$$D = 2^{N-1}, \quad (6)$$

using that for the square lattice the number of plaquettes is equal to the number  $N = L^2$  of lattice sites. The factor  $2^{-1}$  arises because only an even number of sites with nontrivial syndrome  $Z_p = -1$  can exist, as can be seen from the fact that the product of all  $Z_p$  is the identity operator on the torus (all  $Z_b$  appear twice from neighbouring plaquettes and  $\mathcal{Z}_b^2 = 1$ ).

The total number of error patterns is  $2^n$ . And the number of error patterns in an equivalence class is  $2^{N-1}$  because, as explained above, equivalent error patterns are related by  $\tau'_{ij} = \tau_{ij}\sigma_i\sigma_j$ . Each of the  $\sigma_i = \pm 1$  can be chosen independently and gives a different  $\tau'$ , except for an overall reversal of the spin configuration which leaves  $\tau'$  unchanged and gives the factor  $2^{-1}$ . Thus the number of equivalence classes is

$$C = \frac{2^n}{2^{N-1}} = 2^{N+1} \quad (7)$$

which is equal to  $4D$ . This correctly indicates that each syndrome corresponds to four different equivalence classes of error patterns. The above argument easily generalizes to other lattices: in general,  $D = 2^{\mathcal{P}-1}$  where  $\mathcal{P}$  is the number of plaquettes, while  $C = 2^n/2^{N-1} = 2^{n-N+1}$ . The equality  $C = 4D$  then follows from Euler's theorem  $n = \mathcal{P} + N$ .

If we now specify the fraction of errors or error probability  $p$ , most of the  $2^n$  error patterns are excluded

because the number of errors these patterns have is different from  $np$ . Thus the number of equivalence classes containing patterns with  $np$  errors,  $C(p)$ , is significantly smaller than  $C$ . Then the number of syndromes  $D (= 2^{N-1})$  is much larger than  $C(p)$ , and we have a sufficient number of syndromes to specify the equivalence class corresponding to a given syndrome,  $D = C/4 \gg C(p)$ . This implies that a simple number counting does not lead to the critical value  $p_c$  by the classical argument that, beyond  $p_c$ , the number of errors exceeds that of syndromes ( $C(p) > D$ ) and one cannot identify the error from the syndrome, leading to unsuccessful error correction.

### 4. Bounds on Equivalence Classes and Ground-State Energy

We next proceed to evaluate  $C(p)$ . Upper and lower bounds are derived for this quantity, which will further be shown to give a lower bound on the ground-state energy of the  $\pm J$  Ising model.

#### 4.1 Upper bounds

Let us begin by constructing upper bounds. A trivial upper bound for  $C(p)$  is  $C$ ,

$$C(p) \leq C = 2^{N+1} \approx 2^N, \quad (8)$$

where the last expression gives the result to exponential accuracy, which is all we are normally interested in. To derive another upper bound, let us temporarily ignore the equivalence of error patterns, which leads to overcounting. The number of classically distinct error patterns with a fraction  $p$  of errors is

$$\binom{n}{np} \approx 2^{nH(p)}, \quad (9)$$

where  $H(p)$  is the binary entropy,

$$H(p) = -p \log_2 p - (1-p) \log_2 (1-p). \quad (10)$$

We therefore have

$$C(p) \leq 2^{nH(p)} \quad (11)$$

because equivalence will reduce the number by grouping errors into classes. The two upper bounds (8) and (11) cross each other at the point where  $H(p) = \frac{1}{2}$ .

An interesting observation is obtained if we continue to ignore the issue of equivalence and apply the argument for classical codes to the present problem. The number of syndromes is  $D = 2^{N-1} \approx 2^N$ . Thus, if we demand that there exist a sufficient number of syndromes to distinguish all the errors, we have

$$2^{nH(p)} < 2^N. \quad (12)$$

On the square lattice,  $n = 2N$ , and (12) leads to  $H(p) < \frac{1}{2}$  or  $p < 0.1100$  as a necessary condition for classical non-degenerate error correction to be successful. This boundary value  $H(p_c) = \frac{1}{2}$  happens to coincide with the conjecture on the exact location of the multicritical point (separating the ferromagnetic and paramagnetic phases on the NL) of the  $\pm J$  Ising model on the square lattice, which agrees well with numerical estimates (see refs. 2 and 3 and references therein). Somewhat surprisingly, therefore, a naive argument which *ignores* degeneracy nevertheless seems to give the

correct value of the error threshold for the highly degenerate toric code.<sup>1)</sup>

It is also interesting that the lower bound on the existence of generic error-correctable CSS codes, if applied to the toric code, coincides with the above result as pointed out by DKLP.<sup>1)</sup> It is known that there exist CSS codes with critical error probability  $p_c$  and code rate  $R = 1 - 2H(p_c)$  in the asymptotic limit of large code size. Since the toric code has  $R \rightarrow 0$  asymptotically, one finds  $H(p_c) = \frac{1}{2}$ .

#### 4.2 Lower bound (I)

Lower bounds are derived by slightly more elaborate arguments. A loose lower bound is

$$C(p) \geq \frac{2^{nH(p)}}{2^N}. \quad (13)$$

The denominator on the right-hand side is the maximum number of error patterns in an equivalence class, thus leading to a smaller value than  $C(p)$ .

A stronger lower bound is given as

$$C(p) \geq \frac{2^{nH(p_0)}}{2^N}, \quad (14)$$

where  $p_0$  is a function of  $p$  defined by

$$E_g(p_0) = -n(1 - 2p) \quad (15)$$

for sufficiently large  $N$ . Here  $E_g(p_0)$  is the ground-state energy of the  $\pm J$  Ising model with a fraction  $p_0$  of negative bonds in a typical configuration, i.e., one where the positive and negative bonds are randomly distributed. To prove (14), we first recall from above that the number of error patterns for given  $p$ ,

$$A(p) = \sum_{\tau} \delta \left( \sum_{(ij)} \tau_{ij} - E_p \right) = \binom{n}{np} \approx 2^{nH(p)}, \quad (16)$$

where  $E_p = n(1 - 2p)$ , is an overcount of the number of equivalence classes because it ignores equivalence. Each term in (16) should be divided by the number of error patterns equivalent to  $\tau$  which contain the same number of errors:

$$B(p, \tau) = \frac{1}{2} \sum_{\sigma} \delta \left( \sum_{(ij)} \tau_{ij} \sigma_i \sigma_j - E_p \right). \quad (17)$$

The factor  $\frac{1}{2}$  comes from overall up-down symmetry [see before (7)]. We therefore have

$$C(p) = \sum'_{\tau} \frac{\delta \left( \sum_{(ij)} \tau_{ij} - E_p \right)}{B(p, \tau)}. \quad (18)$$

The prime in the sum indicates that terms with  $B(p, \tau) = 0$  should be excluded. Applying a gauge transformation  $\tau_{ij} \rightarrow \tau_{ij} \sigma_i \sigma_j$  and averaging over the gauge variables  $\{\sigma_i\}$  gives, up to an unimportant factor of  $\frac{1}{2}$ ,

$$\begin{aligned} C(p) &= \frac{1}{2^N} \sum'_{\tau} \frac{\sum_{\sigma} \delta \left( \sum_{(ij)} \tau_{ij} \sigma_i \sigma_j - E_p \right)}{B(p, \tau)} \\ &= \frac{1}{2^N} \sum'_{\tau} \frac{B(p, \tau)}{B(p, \tau)} \equiv \frac{1}{2^N} \sum_{\tau} \Theta(B(p, \tau)), \end{aligned} \quad (19)$$

where  $\Theta(x)$  is 1 for  $x > 0$  and 0 for  $x = 0$ . This result is intuitively clear: the final sum in (19) counts all error patterns  $\tau$  for which an equivalent pattern with a fraction  $p$  of errors exists. Every equivalence class contained in  $C(p)$  thus contributes  $2^{N-1} \approx 2^N$  times to the sum, and the prefactor compensates for this.

The lower bound (14) is now obtained by restricting the sum in (19) to typical error patterns  $\tau$  with  $np_0$  errors (i.e.,  $np_0$  negative  $\tau_{ij}$ 's)

$$C(p) \geq \frac{1}{2^N} \sum_{\tau(p_0)} \Theta(B(p, \tau)). \quad (20)$$

For a typical configuration  $\tau$  with  $np_0$  negative bonds,  $B(p, \tau)$  is almost always positive because the constraint on the right-hand side of (17)

$$\sum_{(ij)} \tau_{ij} \sigma_i \sigma_j - E_p = 0 \quad (21)$$

is satisfied by a ground-state configuration of the  $\sigma_i$ , due to the definition of  $p_0$  in (15). We therefore find

$$C(p) \geq \frac{1}{2^N} \binom{n}{np_0} \approx 2^{nH(p_0) - N} \quad (22)$$

which is the lower bound in (14).

#### 4.3 Lower bound (II)

Another lower bound is obtained by restricting the sum in (18) to typical bond configurations  $\tau$  with  $np$  negative bonds (errors). Then  $B(p, \tau)$  is—in spin glass terms—the number of spin configurations with energy  $-E_p = -n(1 - 2p)$  for a typical configuration  $\tau$  with  $np$  negative bonds, the logarithm of which is the thermodynamic entropy on the NL.<sup>6,7)</sup>

$$B(p, \tau) = e^{S(p, \tau)}. \quad (23)$$

Since  $\tau$  is a typical configuration,  $S(p, \tau)$  does not depend on the details of  $\tau$  for sufficiently large system size, so we denote it as  $S(p)$ . Thus the denominator on the right-hand side of (18) can be brought in front of the sum and we find

$$C(p) \geq e^{-S(p)} \sum_{\tau(p)} \delta \left( \sum_{(ij)} \tau_{ij} - E_p \right) \approx 2^{nH(p) - S(p)/\ln 2}. \quad (24)$$

#### 4.4 Behaviour of bounds

Our upper and lower bounds can be summarized as

$$\begin{aligned} &\max(2^{nH(p) - S(p)/\ln 2}, 2^{nH(p_0) - N}) \\ &\leq C(p) \leq \min(2^N, 2^{nH(p)}). \end{aligned} \quad (25)$$

This result is depicted in Fig. 6, where we are using for  $S(p)$  an upper bound from our previous work.<sup>8)</sup> It is seen that  $C(p)$  reaches its maximum value  $2^N$  at some  $p$  below 0.15 and above 0.1100. This is because one of the lower bounds  $2^{nH(p_0) - N}$  reaches the upper bound  $2^N$  at  $p$  close to 0.15. The latter value was obtained by the relation  $nH(p_0) - N = N$  (or  $p_0 = \frac{1}{2}$ ) and using the numerical value of the ground-state energy  $E_g(\frac{1}{2}) = -1.40N$  (see Fig. 7 for this value).

This saturation of the upper bound at an intermediate value of  $p$  is not unnatural because  $C(p)$  is the number of classes of equivalent error patterns, with all classes counted with uniform weight. If we instead give appropriate probability weights to various error patterns, and thence to equivalence classes, we would reach a smaller value, the

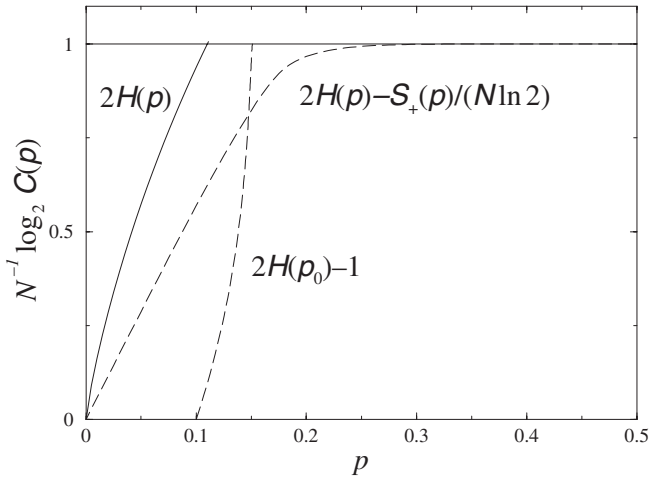


Fig. 6. Upper and lower bounds of  $C(p)$  from (25), plotted as bounds on  $N^{-1} \log_2 C(p)$ . Solid lines give the upper bounds, 1 and  $2H(p)$ , and dashed lines the lower ones,  $2H(p) - S(p)/(N \ln 2)$  and  $2H(p_0) - 1$ . Because  $S(p)$  is not known exactly, we replace it by an upper bound  $S_+(p)$  from our previous study.<sup>8)</sup> To sketch  $2H(p_0) - 1$ , a rough fit was made to the numerical data in Fig. 7 to obtain  $p(p_0)$  and from there the inverse relation  $p_0(p)$ .

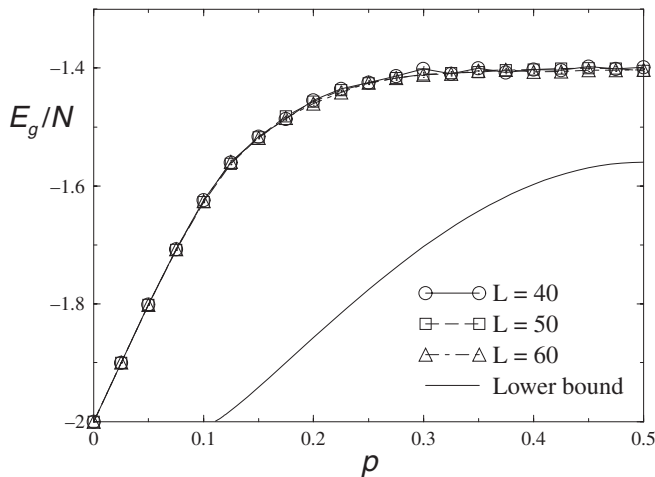


Fig. 7. Ground-state energy of the two-dimensional  $\pm J$  spin glass. Shown is the lower bound resulting from (30), compared with numerical results for linear system sizes  $L = 40, 50$  and  $60$ . The latter were obtained by averaging over 10, 15 and 5 numerical realizations of the disorder, respectively; error bars are smaller than the symbol sizes. All numerical calculations were run on the spin glass ground state server.<sup>10)</sup>

logarithm of which we denote by  $S_\pi$ . Apart from a trivial factor of  $\ln 2$ , this quantity is nothing but the lower bound  $2^{2H(p) - S(p)/\ln 2}$  because the latter was derived by using typical error configurations,

$$S_\pi = nH(p) \ln 2 - S(p). \quad (26)$$

This  $S_\pi$  is of course smaller than the maximum value of  $\ln C(p)$  and reaches its maximum only at  $p = \frac{1}{2}$ .

It is instructive to derive (26) from a different argument. Consider the probability weight of an error pattern  $\tau$  as given in (4). The probability weight of the equivalence class  $\pi$  containing this error pattern is then

$$P_\pi = [p(1-p)]^{n/2} Z_0(p, \tau), \quad (27)$$

where  $Z_0(p, \tau)$  is the partition function (5) for the given  $p$  (on the NL) and  $\tau$ . Then the information-theoretical entropy of the probability distribution  $P_\pi$  of equivalence classes is

$$S_\pi = - \sum_\pi P_\pi \ln P_\pi, \quad (28)$$

which is equal to the information-theoretical entropy of distribution of frustrated plaquettes in the  $\pm J$  Ising model.<sup>8,9)</sup> Using (27) and the relation  $F = -T \ln Z = E - TS$  with  $E = -n(1-2p)$  on the NL, it is possible to reduce this expression to (26). To see this, (28) is first rewritten using (27) as

$$S_\pi = - \frac{n}{2} \ln[p(1-p)] + \frac{E}{T} - S(p). \quad (29)$$

With  $E/T = -n(1-2p) \cdot \frac{1}{2} \ln[(1-p)/p]$  on the NL, we easily recover (26).

We can summarize the difference between  $\ln C(p)$  and  $S_\pi$  as follows. In  $\ln C(p)$  we count (the logarithm of) the total number of different equivalence classes  $\pi$  that can be obtained for given  $p$ , i.e., that have  $P_\pi > 0$ :  $\ln C(p)$  thus measures the size of the *support* of the distribution  $P_\pi$ . On the other hand,  $S_\pi$  is the *entropy* of the distribution, and the fact that it is smaller than  $\ln C(p)$  indicates that the distribution is strongly (i.e., exponentially narrowly) peaked rather than uniformly spread over its support.

#### 4.5 Lower bound on the ground-state energy

The inequality (25) implies the relation

$$nH(p) \geq nH(p_0) - N. \quad (30)$$

If we regard  $p$  as a function of  $p_0$  through the definition  $E_g(p_0) = -n(1-2p)$ , then the above inequality gives a lower bound on  $p(p_0)$ , or equivalently a lower bound on  $E_g(p_0)$ . The result is shown in Fig. 7 together with numerical estimates of  $E_g$ . Our lower bound is not particularly tight numerically, e.g.,  $E_g(p)/N \geq -1.56$  at  $p = \frac{1}{2}$  whereas numerically  $E_g(p)/N$  is around  $-1.40$ . However, this result has non-trivial significance because it is, as far as we know, the first analytical lower bound on the ground-state energy of the two-dimensional  $\pm J$  Ising model with general  $p$ .

## 5. Summary and Discussion

We have derived upper and lower bounds on the number of equivalence classes of error patterns in the toric code. It has been shown that this number saturates its upper bound at an intermediate value of the error probability where we expect no singularities in physical quantities. This apparently non-conventional behaviour has been explained by noting that the number of *typically realized* equivalence classes, which is relevant for physical quantities, is significantly smaller than the number of equivalence classes with uniform weights given to all the cases. The logarithm of the former number has been shown to be equal to the information-theoretical entropy of the probability of error classes, which is further related to the thermodynamic entropy on the NL and therefore has a singularity (albeit a weak one) at the multicritical point.

One of the upper bounds was compared with a lower bound, the latter involving the ground-state energy of the  $\pm J$  Ising model, leading to a lower bound on the ground-state energy of this spin glass model. Although the resulting value

of the lower bound is not necessarily impressive numerically, it is interesting that bounds on the number of equivalence classes of the toric code lead in a simple manner to a bound on the ground-state energy of a spin glass. The correspondence between the two problems was proposed by DKLP,<sup>1)</sup> and we have exploited it here to derive an explicit result on a physical quantity.

The present work would serve as a starting point for further developments based on the correspondence of two completely different problems. For example, an improved upper bound for  $C(p)$  will lead to a better lower bound on the ground-state energy. Improvements of the lower bound of  $C(p)$  may also be possible, but one should remember that such a result may not lead to an improved bound on the ground-state energy unless the obtained lower bound of  $C(p)$  is related to the latter quantity.

### Acknowledgement

We thank John Preskill for very useful discussions and comments on equivalence class in the toric code. We are also grateful to Thomas Lange for technical support with the simulations on the spin glass ground state server. The present work has been supported by the Anglo-Japanese Collaboration Programme by the Japan Society for the

Promotion of Science and The Royal Society. One of the authors (HN) was also supported by the Ministry of Education, Culture, Sports, Science and Technology (MEXT) Grant-in-Aid for Scientific Research on Priority Area ‘Statistical–Mechanical Approach to Information Processing’ and by the MEXT 21st Century COE Programme ‘Nanometer-Scale Quantum Physics’ at Department of Physics, Tokyo Institute of Technology. PS gratefully acknowledges the hospitality of the Tokyo Institute of Technology, where this work was initiated.

- 1) E. Dennis, A. Kitaev, A. Landahl and J. Preskill: J. Math. Phys. **43** (2002) 4452.
- 2) J.-M. Maillard, K. Nemoto and H. Nishimori: J. Phys. A **36** (2003) 9799.
- 3) H. Nishimori and K. Nemoto: J. Phys. Soc. Jpn. **71** (2002) 1198.
- 4) A. R. Calderbank and P. W. Shor: Phys. Rev. A **54** (1996) 1098.
- 5) A. Steane: Proc. R. Soc. London, Ser. A **452** (1996) 2551.
- 6) H. Nishimori: Prog. Theor. Phys. **66** (1981) 1169.
- 7) H. Nishimori: *Statistical Physics of Spin Glasses and Information Processing: An Introduction* (Oxford University Press, Oxford, 2001).
- 8) H. Nishimori and P. Sollich: *Frontiers in Magnetism*, J. Phys. Soc. Jpn. **69** (2000) Suppl. A, p. 160.
- 9) H. Nishimori: J. Phys. Soc. Jpn. **55** (1986) 3305.
- 10) The Spin Glass Ground State Server: [http://www.informatik.uni-koeln.de/ls\\_juenger/research/sgs/sgs.html](http://www.informatik.uni-koeln.de/ls_juenger/research/sgs/sgs.html)